NASA TECHNICAL MEMORANDUM

NASA TM X-71885

NASA TM X-71885

CLOSED CYCLE MHD POWER GENERATION EXPERIMENTS USING A HELIUM-CESIUM WORKING FLUID IN THE NASA LEWIS FACILITY

by Ronald J. Sovie
Lewis Research Center
Cleveland, Ohio 44135

TECHNICAL PAPER to be presented at
Fifteenth Symposium on the Engineering
Aspects of Magnetohydrodynamics
Philadelphia, Pa, May 24-26, 1976

CLOSED CYCLE MHD POWER GENERATION EXPERIMENTS USING A HELIUM-CESIUM WORKING FLUID IN THE NASA LEWIS FACILITY

Ronald J. Sovie
NASA Lewis Research Center
Cleveland, Ohio 44135

E-8660

ABSTRACT

Since the last EAM Symposium, the MHD channel, which was previously operated for over 500 hours of thermal operation, ten thermal cycles, and 200 cesium injection tests, was removed from the facility and redesigned. The cross sectional dimensions of the channel were reduced to 5 by 16.5 cm to allow operation over a variety of conditions. The redesigned channel has been operated for well over 300 hours, 10 thermal cycles, and 150 cesium injection tests with no problems. Experiments have been run at temperatures of 1900-2100 K and Mach numbers from 0.3 to 0.55 in argon and 0.2 in helium. The ability to run over a variety of conditions coupled with improvements in Hall voltage isolation and seed vaporization techniques have increased our understanding of the generator phenomena and have resulted in significant improvements in performance. The best results to date have been obtained in the helium tests. Typical values obtained with helium are Faraday open circuit voltage V_{FOC} = 141 V (92% of uBh) at B = 1.7 T, power outputs of 2.2 kw for tests with 28 electrodes and 2.1 kw for tests with 17 electrodes Power densities of 0.6 MW/m^3 and Hall fields of ∿1100 V/m were obtained in the tests with 17 electrodes. These results represent a factor of ∿18 improvement in power density over the previously reported results. However, the V-I curves and current distribution data indicate that while near ideal equilibrium performance is obtained under some conditions, no non-equilibrium power has been generated to date.

I. INTRODUCTION

The goal of the NASA Lewis closed cycle MHD program is to demonstrate non-equilibrium performance at temperatures of ∿2000 K and power densities of 1-10 MW/m^3 for periods ranging from a few minutes to steady state. The closed loop facility is operated continuously with hot generator walls (∿1900 K) to better simulate the conditions under which a real generator must perform. This program complements the very short duration shock tube experiments aimed at demonstrating large enthalpy extraction ratios and reasonable turbine efficiencies,[1,2] and the blowdown experiments which have been carried out in Frascati.[3]

The successful demonstration of non-equilibrium MHD performance in a closed loop steady-state system could lead to lighter space power generation systems and higher efficiency ground power generation systems.[4] In the latter case, the heat source for the MHD generator could be an advanced gas cooled reactor or a fossil fuel-fired combustion heat exchanger system.[5]

The achievement of our performance goal requires solution not only of the basic plasma physics problems associated with obtaining good MHD generator performance, but also the problems associated with: a) design and construction techniques for good generator performance and lifetime, b) materials lifetime and compatibility, c) systems component compatability, d) electrode effects, e) Hall shorting phenomena, f) cesium seeding system behavior, and g) obtaining general overall system integrity. During the past year we have made some progress toward obtaining good MHD generator performance and have reached the point of overall system integrity that allows us now to direct our main efforts towards the plasma physics problems.

In the present mode of operation, the inert gas loop operates in the steady state, When the system is at the operating temperature (1900-2100 K) a series of cesium injection tests of duration between 10 seconds and a few minutes are made. Once satisfactory MHD performance is obtained in this mode of operation, the emphasis of the program will shift to making long duration cesium injection tests.

Since the 14th EAM Symposium, the cross sectional dimensions of the channel were reduced to 5 by 16.5 cm. The redesigned channel has been operated for well over 300 hours, 10 thermal cycles, and 150 cesium injection tests with no problems and has allowed operation over a range of conditions. The results of tests using a helium-cesium working fluid at gas stagnation temperature of 2000 K and a Mach number of 0.21 will be presented in this paper.

II. FACILITY

Only a brief description of the facility will be given in this section; a more detailed description is contained in Ref. 6.

Figure 1 is a schematic of the closed loop facility. The gas leaving the compressor is preheated in a parallel-flow recuperative heat exchanger (preheater) before entering the graphite resistance heater. On leaving the heater through the nozzle the hot gas enters the MHD channel, expands in the diffuser, and enters the shell side of the preheater. Conventional equipment is used to further cool, dry, and filter the gas as it flows toward the compressor. Typical gas temperatures at various points in the loop and the efficiencies of various loop components are indicated in Fig. 1.

The preheater is grounded. In order to obtain proper ground isolation, all other components that can see the plasma are isolated from ground. The cesium is injected in the heater end bell. A series of horizontal and vertical mixing bars are placed between the nozzle exit and duct entrance.

The heater consists of an outer water-cooled stainless steel shell, a lining of high density castable refractory cement, and four graphite heater elements surrounded by magnesium oxide bricks. The heater has been run for 1600 hours without maintenance at power levels up to 1.4 MW. The main problem with the heater has been to isolate it from ground at peak system temperatures

during cesium injection tests. The heater has been run at 550 V below ground, but intermittent electrical breakdowns occur at higher generated Hall voltages.

A schematic representation of the MHD channel is shown in Fig. 2. The channel cross sectional area is 6.35 by 20 cm at the ends and is reduced to 5 by 16 cm in the 70 cm electrode region. The probes P1 and P2 serve as Hall voltage probes and can be shorted through an ammeter to measure the Hall current in diagnostic tests. There are 28 pairs of thoriated tungsten electrodes on 2.54 cm centers located in the middle of the 91.4 cm long magnetic field region.

The cesium is injected 71 cm upstream of the MHD channel in the heater end bell region. The cesium injection system consists of a molybdenum storage plenum and a series of molybdenum injection tubes all located in the heater end bell. The system is operated in two modes. A continuous mode where a monitored cesium flow is continuously injected into the system under pressure and a blowdown mode where a measured amount of cesium is injected into the plenum, stored for a short duration and then blown out using high pressure helium. The blowdown tests last from 10-20 seconds and the MHD performance is significantly improved in this mode of operation. Realistically, the exact quality of the cesium vapor and hence the exact cesium seed rate must be treated as an unknown in either mode of operation.

III. EXPERIMENTAL PROGRAM

Background

The two main problems which have adversely affected our MHD performance in the past have been poor cesium seed quality and the presence of low resistance Hall current leakage resistance paths during cesium injection tests.[7,8] The Hall current leakage path was found to be due to a ground loop that was present only during cesium injection. As was previously mentioned, the preheater tubes in the channel exit region are grounded and cannot be readily floated. So in an effort to reduce the ground loop leakage resistance, we have redoubled our efforts to isolate the high-temperature components (heater, duct, etc.) from ground and from each other.

In order to obtain a better seed quality, a molybdenum cesium storage plenum was added in the heater end bell region, and the cesium system is run in the blowdown mode described in the previous section. This mode of operation results in higher vapor seed rates and significant improvements in performance over the steady-state seed injection. However, the actual vapor seed fraction must be treated as an unknown in this mode of operation.

In the past year, tests were conducted using a helium-cesium working fluid. The use of helium allows operation at higher velocities and hence higher Faraday voltages. The lower electron mobility in helium can also alleviate the Hall shorting phenomena.

Tests were run under a variety of load conditions using all 28 electrode pairs or using a configuration in which the first 17 electrode pairs were loaded and the last 11 were open circuited. The purposes of the 17 electrode tests were twofold. First, the magnetic field region in the open circuited area increases the resistance between the last loaded electrode and the grounded preheater tubes. Secondly, if a Hall leakage current does flow from the loaded electrodes to ground, the change in the measured open circuit voltage of the last few electrodes over that measured when all the electrodes are run open circuited can be used to determine the value of the leakage current. This information is necessary because simultaneous measurement of the Faraday current, Hall voltage, and Hall leakage current is necessary in order to determine the vapor seed fraction, S_v, using the data analysis theory in Ref. 9. The theory used is an extension of the results of Dzung[10] and includes the effects of finite electrode segmentation, electrode voltage drops, and leakage resistances in the Hall and Faraday directions.

IV. EXPERIMENTAL RESULTS

Operating Conditions

The operating conditions for the data presented herein were gas stagnation temperature T_s = 2000 K, gas stagnation pressure $P_s = 1.42 \times 10^5$ N/m^2, helium mass flow rate $\dot{M}_{He}$ = .146 kg/s, Mach number M = 0.21, velocity u = 543 m/s and uh = 89.6 V/T.

Faraday Open Circuit Voltage Behavior

The variation in the measured Faraday open circuit voltage V_{FOC} along the channel length is shown in Fig. 3. The Faraday voltages are seen to be quite uniform for the center 20 electrode pairs. The front end behavior is a Faraday shorting effect due to the presence of a set of pre-ionizer electrodes. The apparent degradation of the voltage at the last four electrode pairs is caused by a change in the electrode separation which was done purposely to test some boundary layer effects.

The ratio of the measured Faraday open circuit voltage at electrode pair 15 to the ideal uBh is plotted versus the magnetic field strength in Fig. 4. The figure shows that the measured V_{FOC} is 92 percent of the ideal voltage or higher for magnetic field strengths up to 1.7 T. The data indicates that the electrical integrity of the hot walls in the Faraday direction is quite good.

Behavior at Short Circuit and Load Conditions

Tests were run at various magnetic field strengths using both the 17 and 28 electrode configurations and various values of the load resistance R_L. The current distribution along the channel length for B = 1.48 T is shown for R_L = 0 and R_L = 40 for the 17 electrode tests and for R_L = 40 for a 28 electrode test on Fig. 5. The figure shows that with the exception of end effects, the current distribution along the channel is quite uniform. The end effect is seen to be more pronounced at short circuit conditions and in the 17 electrode tests. These current profiles are typical of those obtained at other magnetic field strengths.

The voltage-current curves obtained for magnetic strengths of 1.04, 1.48, and 1.68 T for a typical set of electrodes are shown in Fig. 6. The uniform variation of the V-I curves and the lack of

a pronounced increase in the Faraday current along the channel length indicate that the performance is equilibrium MHD performance. No significant non-equilibrium ionization effects have been observed in our experiments to date.

The variation of the measured Faraday voltages along the channel length for a test in which B = 1.68 T is shown in Fig. 7. Three sets of data are shown for this test. The open circuit voltage was measured for all 28 electrode pairs. The first 17 electrodes were then loaded with 40 Ω resistances and data taken in the uniform seed blowdown period (squares) with 17 loaded electrodes and the last 11 open circuited. The final set (triangles) was taken near the end of the blowdown period when the vapor seed fraction, S_v, was decreasing. The open circuit voltage distribution for the 28 electrodes and load voltage distribution for the 17 electrodes are seen to be similar to the distributions shown in Figs. 3 and 5, respectively. The figure also shows that the open circuit voltages in the 17 electrode tests recover to a reasonable uniform value 5 to 6 electrode pairs downstream of the last electrode pair in which current flows. The measured V_{FOC} for the last four electrodes is also seen to be decreased from the value obtained when all 28 electrodes are open circuited. This change in voltage ΔV_{FOC} is assumed to be caused by the flow of the Hall leakage current, I_x. The vapor seed fraction, S_v, and Hall leakage current I_x determined from the data analysis must then satisfy the condition

$$\Delta V_{FOC} = \frac{\mu_e(S_v)}{\sigma(S_v)} \frac{I_x}{A_x} hB$$

where μ_e = the electron mobility, σ = electrical conductivity, h = channel height, and A_x is the channel cross-sectional area. For cases when all 28 electrodes are loaded, it is assumed that all the leakage flows through the plasma to the grounded preheater tubes. In this case, the calculated S_v and I_x must satisfy the condition that the measured voltage of probe 2 to ground (see Fig. 2) is $Vp2 = I_x R_{p2G}(S_v)$.

Figure 7 shows that ΔV_{FOC} = 5-6 V for the data at the normal blowdown conditions and ∿7 V for the data taken near the end of the blowdown period. Values as high as 40 V have been measured for cases when a breakdown of the resistance of the high temperature components to ground occurred and the Hall shorting problems were severe. It is also seen that the power output is reduces from 1.75 kW to 0.76 kW near the end of the blowdown period when the seed fraction is diminished. The variation of the Hall voltage along the channel length for the same data points is shown in Fig. 8. The Hall voltage is plotted with respect to ground and the load resistance was 40 Ω. The figure shows that some Hall voltage is generated in the region between probe 1 and electrode 1 as one would expect from the front end effect exhibited by the current profiles. The voltages of the heater and vaporizer (H and V on the figure) to ground are nearly identical to that of probe 1 indicated that the flow of Hall leakage currents through the plasma to these elements is small. The figure also shows that the measured Hall voltage is much higher for the data near the end of the seed blowdown period when the seed fraction is reduced.

The maximum Hall voltage generated to date was measured at the end of the cesium blowdown and was 550 V for $R_L = 0$ and B = 1.7 T.

Representative data and results for the helium-cesium tests are given in table I. The Faraday voltages, currents, power output, and Hall voltages are measured quantities. The vapor seed fraction S_v, Faraday resistance R_y, Hall leakage resistance R_x, and Hall leakage current I_x have been calculated using the data analysis theory,[9] the measured currents and voltages, the known run conditions, and the above mentioned boundary conditions on I_x and S_v. The Faraday resistance R_y is the total resistance that the generator sees. The effect of Faraday leakage resistances can be neglected under load condtions and R_y is treated as the sum of the load resistance and a resistance associated with the electrode voltage drop. This voltage drop is calculated as $I_y[R_y - R_L]$ and is also listed in table I. The last two columns compare the measured Faraday current, and Hall voltage with the ideal equilibrium values i.e. those calculated for $R_y = R_L$ and $R_x = \infty$.

The results in table I show that there is a run-to-run variation in seed fraction and Hall leakage resistance for the normal blowdown data (runs without an a in the remarks column). S_v is in the range 0.34 to 0.56 percent for these runs and σ and μ_e are not sensitive functions of S_v in this range of values. However, the variation in the Hall leakage resistance can make a run-to-run comparison difficult. In spite of these variations it is seen that the power per electrode is highest for the load factors nearest 0.5 and that the equivalent power determined from short circuit runs is equal to the actual power measured when K = 0.5. The equivalent power for the $R_L = 0$ cases is roughly proportioned to B^2 although this is not true for all the loaded cases.

The values of the Hall leakage resistances are in the range 200-400 Ω for the normal blowdown rests and reasonably high fractions of the ideal equilibrium performance are obtained for these tests. For the data sets taken near the end of the blowdown period, the seed fraction is reduced by about 1/4. The reduction in power output for this condition appears to be caused by an increase in the electrode voltage drop.

V. DISCUSSION OF RESULTS

The results presented in the previous sections show that we obtain excellent open circuit voltage behavior and reasonable fractions of the ideal equilibrium performance under load conditions. The goal of the program is, however, to obtain non-equilibrium performance and we have not as yet observed any non-equilibrium effects. Nevertheless the initial results obtained in the helium-cesium tests have been quite encouraging. Power outputs of ∿120 W/electrode and power densities of ∿0.6 MW/m^3 have been obtained. The best previously reported performance was a power output of 280 watts for the whole channel and a power density of ∿.035 MW/m^3 for the argon-cesium tests.

The use of the helium-cesium working fluid allows us to run at higher gas velocities thus increasing the Faraday voltages and the magnitude of the ideal equilibrium performance. Improvements in the Hall voltage isolation (previous R_x values ≳ 80-100) and seed system performance have

resulted in our obtaining higher fractions of the ideal equilibrium performance. These are the major reasons for the increased values of the generated power output and power density.

VI. CONCLUDING REMARKS

Tests run with a helium-cesium working fluid have resulted in substantial improvements over the previous results obtained with the argon-cesium working fluid. These improvements were mainly due to the higher voltages obtained with helium, improvements in the seed injection system and better Hall voltage isolation.

The MHD channel is presently being modified so that the channel dimensions will be 11.4 by 3.8 cm in the electrode area. This change will allow operation at Mach numbers up to ∿0.5 in helium and will increase the maximum Faraday field from the present 1000 V/m to ∿2100 V/m. This change and further improvements in the electrical isolation of the high temperature components may result in the non-equilibrium MHD performance.

VII. REFERENCES

1. Tate, E., Marston, C. H., and Zauderer, B., "Large Enthalpy Extraction Resu'ts in a Non-Equilibrium MHD Generator," Sixth International Conference on Magnetohydrodynamic Electrical Power Generation, Internl. Atomic Energy Agency, Vienna, 1975, Vol. III, pp. 89-104.

2. Blum, J., et al., "High Power Density Experiments in the Eindoven Shock Tunnel MHD Generator," Sixth International Conference on Magnetohydrodynamic Electrical Power Generation, Internl. Atomic Energy Agency, Vienna, 1975, Vol. III. pp. 73-88.

3. Gasparotto, M., et al., "Recent Results of Nonequilibrium MHD Generator Experiments in the CNEN Blowdown Loop Facility," Sixth International Conference on Magnetohydrodynamic Electrical Power Generation, Incernl. Atomic Energy Agency, Vienna, 1975, Vol. III, pp. 47-62.

4. Seikel, G. R., and Nichols, L. D., "The Potential of Nuclear MHD Electric Power Systems," AIAA Paper No. 71-638, presented at 7th Propulsion Joint Specialist Conference, Salt Lake City, Utah, June 14-18, 1971.

5. Zauderer, B., et al., "Blowdown Test Facility for a Fossil Fueled Nonequilibrium MHD Generator," Proceedings of the 13th Symposium on the Engineering Aspects of Magnetohydrodynamics, M. Mitchner, ed., Mississippi Univ. Press, 1973, pp. IV.3.1-IV.3.-6.

6. Sovie, R. J., and Nichols, L. D., "Status of Power Generation Experiments in the NASA Lewis Closed Cycle MHD Facility," AIAA Paper No. 72-103, presented at 10th Aerospace Sciences Meeting, San Diego, California, January 17-19, 1972.

7. Sovie, R. J. and Nichols, L. D., "Results Obtained in NASA Lewis Closed Cycle Magnetohydrodynamic Power Generation Experiments," NASA TM X-2277 (Apr. 1971).

8. Sovie, R. J. and Nichols, L. D., "Closed Cycle Power Generation Experiments in the NASA Lewis Facility," Proceedings of the 14th Symposium on the Engineering Aspects of Magnetohydrodynamics. Y.C.L. Wu, ed., Mississippi Univ. Press, 1974, pp. VII.6.1-VII.6.6.

9. Nichols, L. D. and Sovie, R. J., "Hall Current Effects in the NASA Lewis Magnetohydrodynamic Generator," NASA TM X-2606 (Jul. 1972).

10. Dzung, L. S., "Influence of Wall Conductance on the Performance of MHD Generators with Segmented Electrodes," Symposium on Magnetohydrodynamic Electrical Power Generation; Electricity From MHD, International Atomic Energy Agency, Vienna, 1966, Vol. II, pp. 169-176.

TABLE I. - TYPICAL RESULTS FOR HELIUM-CESIUM TESTS

[Run conditions T_s = 2000 K, P_s = 1.42x10^5 N/m^2, $\dot{M}_{He}$ = 0.16 kg/s, u = 543 m/s.]

Run no.	Remarks	Magnetic field strength, B, T	Number of electrodes	Load resistance		Faraday voltage, V_F, V	Faraday current, I_y, A	Power per electrode, P/el, W	Total power, P, kW	Power per unit volume, P/v MW/m^3	Hall voltage, V_x, V	Hall field, E_x, V/M	Calculated vapor seed fraction, S_v, %	Calculated Faraday resistance, R_y, Ω	Calculated Hall resistance, R_x, Ω	Calculated Hall leakage current, I_x, A	Calculated electrode voltage drop, $I_y[R_y-R_L]$ V	Fraction of ideal equilibrium values,	
				R_L,	Load factor, K													I_y/I_{yID}	V_x/V_{xID}
47-10		1.04	17	40	0.49	44.4	1.11	49	0.83	0.23	95	228	0.41	51.5	193	0.49	12.8	0.82	0.78
47-10	a	1.04	17	40	.37	33.5	0.84	28	.48	0.13	140	337	0.11	66	467	0.30	21.8	0.73	0.70
47-11	b,c	1.04	17	0	----	----	2.35	52.8	0.90	0.25	195	470	-----	-----	---	-----	----	----	----
47-1		1.48	17	100	.7	87.5	0.875	76.6	1.30	0.36	93	224	0.5	112	296	0.316	10.5	0.88	0.88
47-2		1.48	17	70	.6	74	1.06	78.4	1.33	0.37	136	328	0.39	86.7	300	0.45	18	0.81	0.80
47-3		1.48	17	40	.48	60.5	1.51	92	1.56	0.44	180	434	0.45	53	366	0.49	19.6	0.81	0.80
47-5	b,c	1.48	17	0	----	----	2.9	92	1.56	0.44	330	795	-----	-----	---	-----	----	----	----
47-13		1.48	28	40	.44	54.7	1.37	75	2.02	0.36	300	438	0.34	56	262	1.14	21.9	0.76	0.68
47-7		1.68	17	70	.56	79.4	1.13	90	1.53	0.43	150	361	0.46	92	242	0.62	24.9	0.78	0.73
47-6		1.68	17	40	.46	64.2	1.61	103	1.75	0.49	205	493	0.50	56	271	0.76	25.7	0.76	0.72
47-6	a	1.68	17	40	.31	42.4	1.12	45	0.76	0.21	310	747	0.11	80	830	0.37	44.8	0.65	0.63
47-9	b,c	1.68	17	0	----	----	3.34	117	1.99	0.56	395	952	-----	-----	---	-----	----	----	----
47-8		1.68	28	70	.51	72.8	1.04	76	2.12	0.36	240	350	0.408	100	214	1.11	31.2	0.72	0.66
47-17	b,c	1.71	17	0	----	----	3.46	121	2.06	0.58	405	976	-----	-----	---	-----	----	----	----
47-17	a,b,c	1.71	17	0	----	----	2.44	85	1.45	0.41	435	1048	-----	-----	---	-----	----	----	----

[a] Data taken near end of blowdown period.
[b] Due to an error in data taking procedure data analysis could not be done for short circuit cases.
[c] Power defined as $P = 1/4\ V_{FOC}I_{FSC}$.

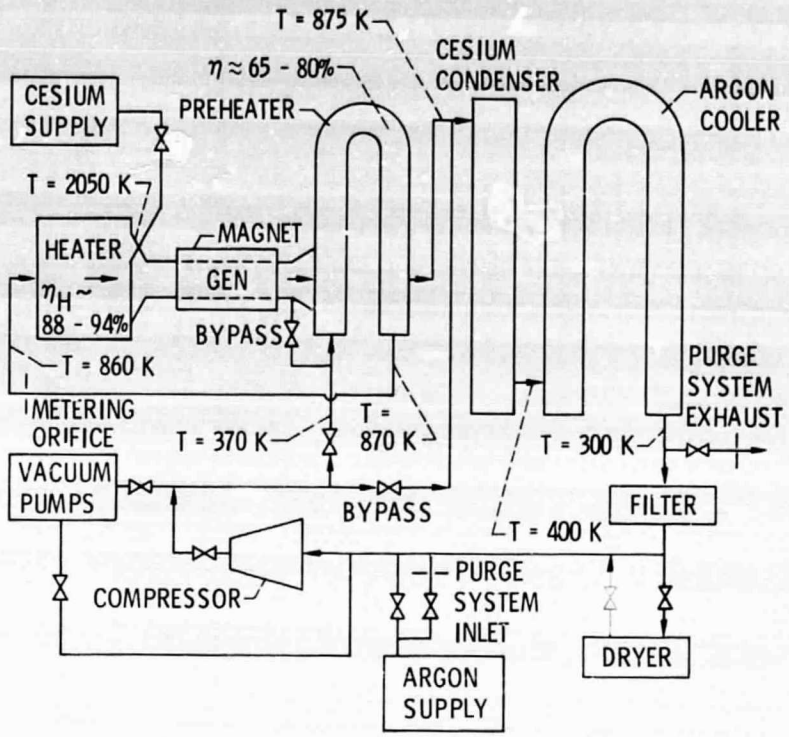

Figure 1. - Loop schematic.

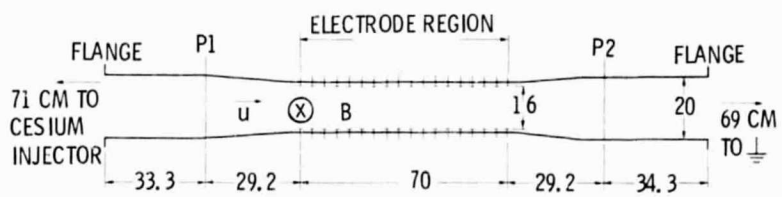

Figure 2. - Schematic representation of MHD channel (all dimensions are in cm.) Channel width = 6.35 cm, reduced to 5 cm in electrode area.

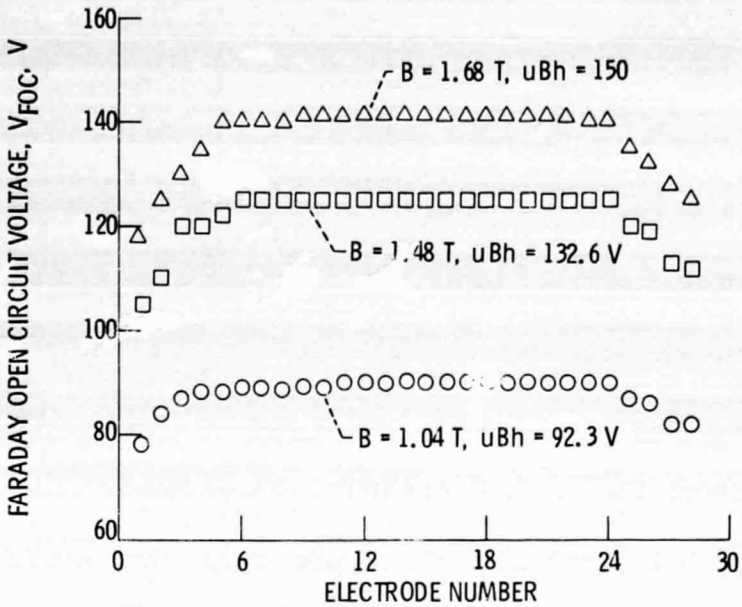

Figure 3. - Variation of Faraday open circuit voltage along the channel.

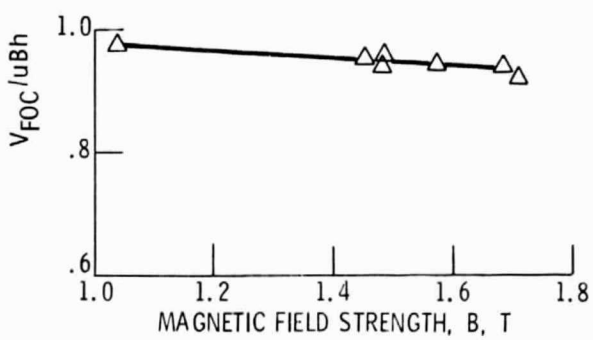

Figure 4. - Ratio of Faraday Open circuit voltage, V_{FOC} to uBh versus magnetic field strength, B.

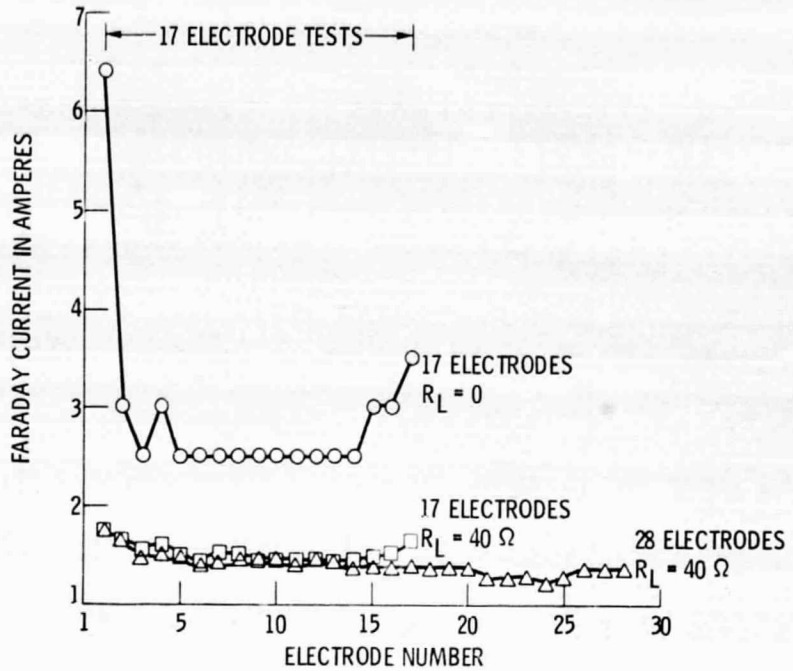

Figure 5. - Distribution of Faraday current along the channel B = 1.48 T.

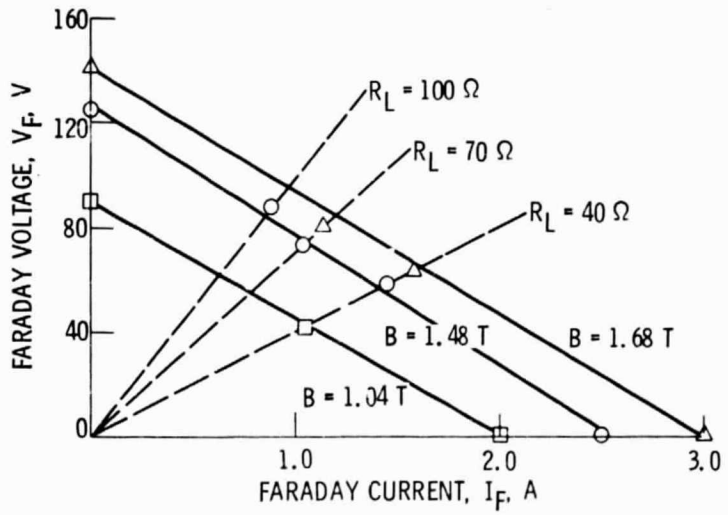

Figure 6. - Voltage-current curves for various magnetic field strengths.

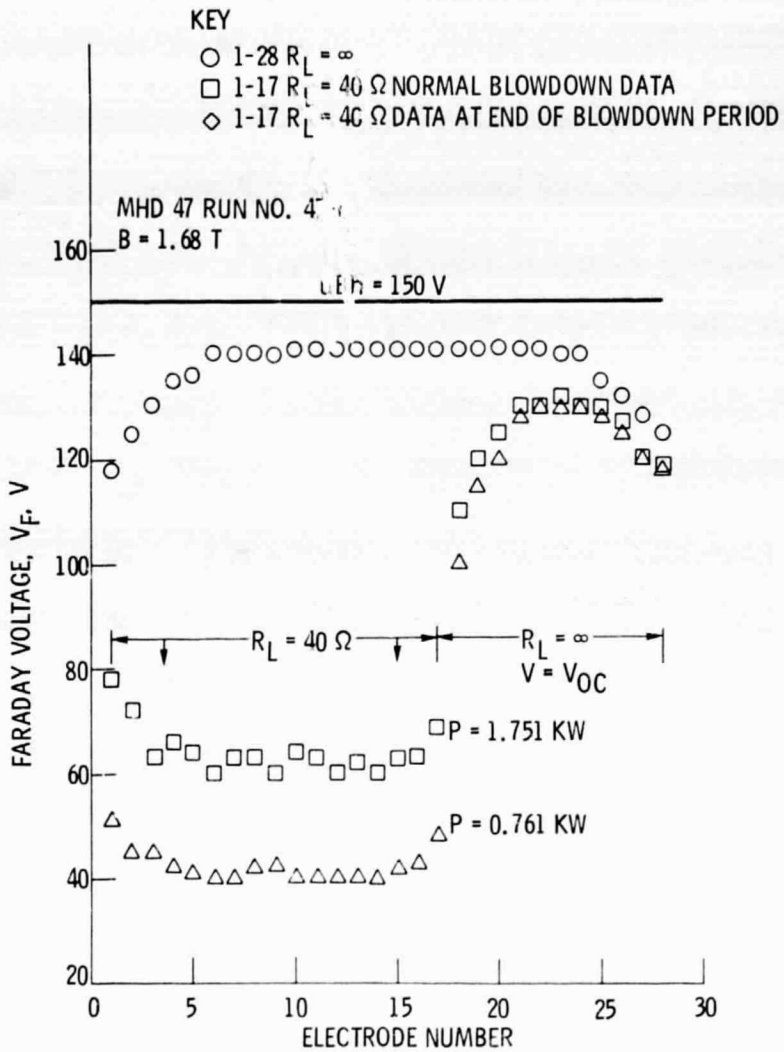

Figure 7. - Variation of Faraday voltage along the channel for B = 1.68 T.

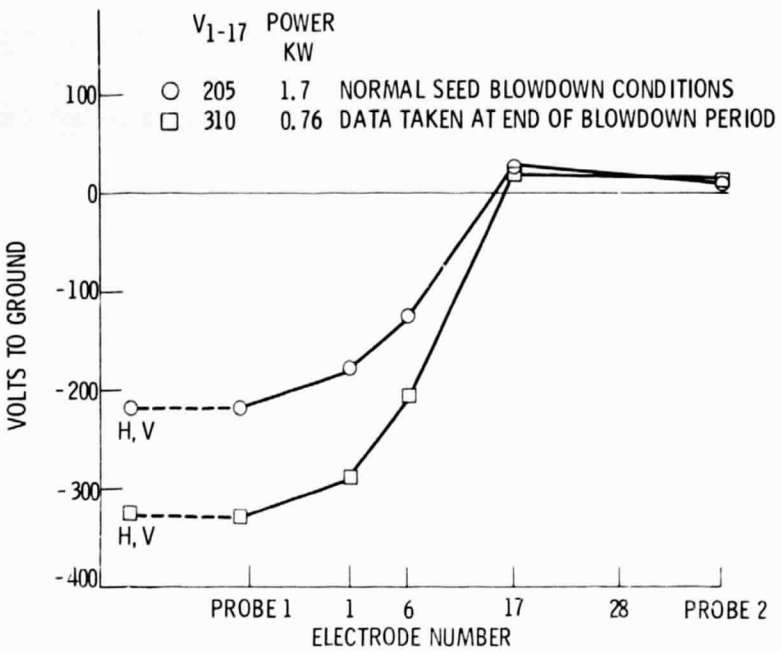

Figure 8. - Variation of Hall voltage along th channel for B = 1.68 T, R_L = 40 Ω.